CHAPTER 4. ATMOSPHERIC TRANSPORT

We saw in chapter 3 that air motions play a key role in determining the distributions of chemical species in the atmosphere. These motions are determined by three principal forces: gravity, pressure-gradient, and Coriolis. We previously saw in chapter 2 that the vertical distribution of mass in the atmosphere is determined by a balance between gravity and the pressure-gradient force; when these forces are out of balance *buoyant motions* result, which will be discussed in section 4.3. In the horizontal direction, where gravity does not operate, the equilibrium of forces usually involves a balance between the pressure-gradient force and the Coriolis force, and the resulting steady flow is called the *geostrophic flow*. Below 1-km altitude, the horizontal flow is modified by friction with the surface.

The atmosphere is considerably thinner in its vertical extent (scale height 7 km) than in its horizontal extent. The largest scales of motion are in the horizontal direction and form the basis for the *general circulation* of the atmosphere. We will concern ourselves first with these horizontal motions.

4.1 GEOSTROPHIC FLOW

Large-scale movement of air in the atmosphere is driven by horizontal pressure gradients originating from differential heating of the Earth's surface (recall our discussion of the sea breeze effect in section 2.5). As air moves from high to low pressure on the surface of the rotating Earth, it is deflected by the *Coriolis force*. We begin with an explanation of the Coriolis force and then go on to examine the balance between the pressure-gradient and Coriolis forces.

4.1.1 Coriolis force

Consider an observer fixed in space and watching the Earth rotate. From the perspective of the observer, an object fixed to the Earth at latitude λ is traveling in a circle at a constant translational speed in the longitudinal direction

$$v_E = \frac{2\pi R \cos\lambda}{t} \qquad (4.1)$$

where t = 1 day (Figure 4-1). For $\lambda = 42^o$ (Boston) we find v_E = 1250

km h^{-1}. We are oblivious to this rapid motion because everything in our frame of reference (these notes, your chair...) is traveling at the same speed. Note that v_E decreases with increasing latitude; it is this latitudinal gradient that causes the Coriolis force.

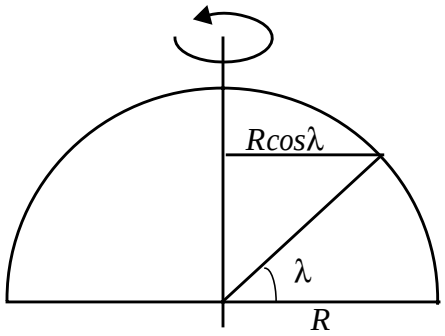

Figure 4-1 Spherical geometry of Earth

Consider now an observer *O* fixed to the Earth and throwing a ball at a target *T*. To begin with the simplest case, imagine the observer at the North Pole and the target at a lower latitude (Figure 4-2). It takes a certain time Δt for the ball to reach the target, during which time the target will have moved a certain distance Δx as a result of the Earth's rotation, causing the ball to miss the target.

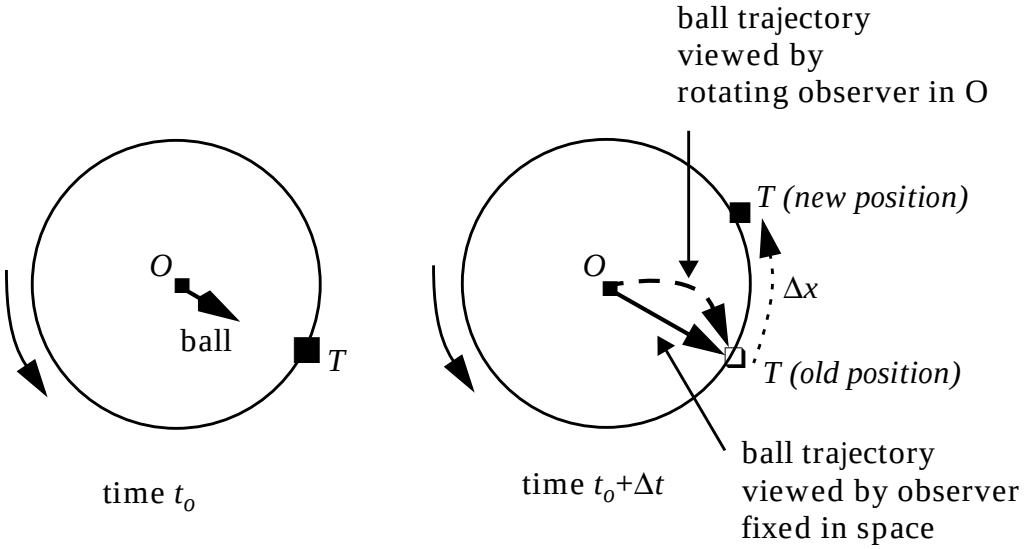

Figure 4-2 Coriolis effect for rotating observer at North Pole

The rotating observer at the North Pole does not perceive the target as having moved, because everything in his/her frame of reference is moving in the same way. However, the shot missed. From the perspective of this observer, the ball has been deflected to the right of the target. Such a deflection implies a force (the Coriolis force)

exerted to the right of the direction of motion. An observer fixed in space over the North Pole notices no such deflection (Figure 4-2). Thus the Coriolis force is fictitious; it applies only in the rotating frame of reference. However, we must take it into account because all our atmospheric observations are taken in this rotating frame of reference.

Let us now consider the more general case of an observer fixed to the Earth at latitude λ_1 in the northern hemisphere and throwing a ball at a target located at a higher latitude λ_2 (Figure 4-3).

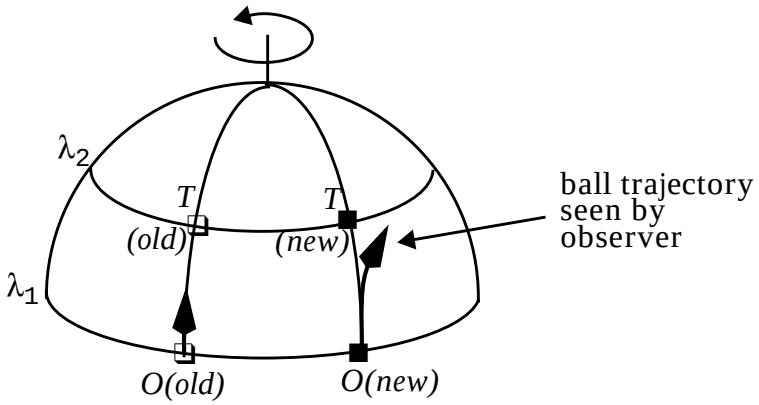

Figure 4-3 Coriolis effect for meridional motion

As the ball travels from λ_1 to λ_2 it must conserve its angular momentum $mv_E(\lambda_1)R\cos\lambda_1$ where m is the mass of the ball, $v_E(\lambda_1)$ is the translational velocity of the Earth at λ_1, and $R\cos\lambda_1$ is the radius of rotation at λ_1. Since $v_E(\lambda_2) < v_E(\lambda_1)$, conservation of angular momentum necessitates that the ball acquire an eastward velocity v relative to the rotating Earth by the time it gets to latitude λ_2. Again, from the perspective of the rotating observer in O the ball has been deflected to the right. By the same reasoning, a ball thrown from λ_2 to λ_1 would also be deflected to the right.

The Coriolis force applies similarly to longitudinal motions (motions at a fixed latitude). To show this, let us first consider a ball at rest on the Earth's surface. From the perspective of an observer fixed to the Earth's surface, the ball experiences a centrifugal force perpendicular to the axis of rotation of the Earth. This force is balanced exactly by the acceleration of gravity and by the reaction from the surface (Figure 4-4). Because the Earth is not a perfect sphere, gravity and reaction do not simply oppose each other. The non-sphericity of the Earth is in fact a consequence of

the centrifugal force applied to the solid Earth; we should not be surprised that the forces of gravity and reaction applied to an object at rest on the Earth's surface combine to balance exactly the centrifugal force on the object.

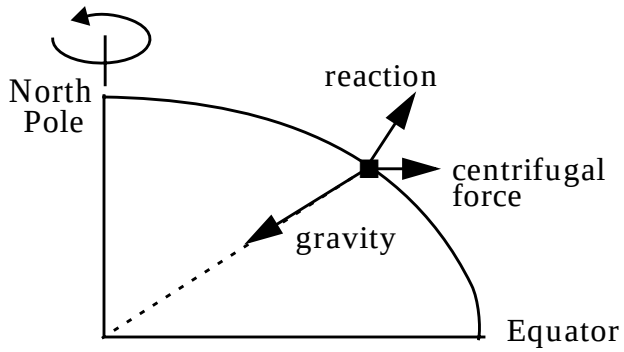

Figure 4-4 Equilibrium triangle of forces acting on a ball at rest on the Earth's surface. The non-sphericity of the Earth is greatly exaggerated.

Let us now throw the ball from west to east in the northern hemisphere. Since the ball is thrown in the direction of the Earth's rotation, its angular velocity in the fixed frame of reference increases; it experiences an increased centrifugal force. As can be seen from Figure 4-4, the increase in the centrifugal force deflects the ball towards the Equator, i.e., to the right of the direction of motion of the ball. Conversely, if the ball is thrown from east to west, its angular velocity in the fixed frame of reference decreases; the resulting decrease in the centrifugal force causes the ball to be deflected towards the pole, again to the right of the direction of motion.

We can generalize the above results. An object moving horizontally in any direction on the surface of the Earth experiences (from the perspective of an observer fixed to the Earth) a Coriolis force perpendicular to the direction of motion, to the right in the northern hemisphere and to the left in the southern hemisphere. Convince yourself that the Coriolis force in the southern hemisphere indeed acts to deflect moving objects to the left. One can derive the Coriolis acceleration γ_c applied to horizontal motions:

$$\gamma_c = 2\omega v \sin\lambda \qquad (4.2)$$

where ω is the angular velocity of the Earth and v is the speed of the moving object in the rotating frame of reference (not to be confused with v_E, the translational speed of the Earth). The Coriolis force is zero at the equator and increases with latitude (convince yourself from the above thought experiments that the Coriolis force must indeed be zero at the equator). Note also that

the Coriolis force is always zero for an object at rest in the rotating frame of reference ($v = 0$).

The Coriolis force is important only for large-scale motions. From equation *(4.2)* we can calculate the displacement ΔY incurred when throwing an object with speed v at a target at distance ΔX:

$$\Delta Y = \frac{\omega(\Delta X)^2 \sin\lambda}{v} \tag{4.3}$$

At the latitude of Boston (42^0N), we find that a snowball traveling 10 m at 20 km h^{-1} incurs a displacement ΔY of only 1 mm. By contrast, for a missile traveling 1000 km at 2000 km h^{-1}, ΔY is 100 km (important!). In the previously discussed case of the sea-breeze circulation (section 2.5), the scale of motion was sufficiently small that the Coriolis effect could be neglected.

4.1.2 Geostrophic balance

We saw in chapter 2 that a pressure gradient in the atmosphere generates a *pressure-gradient force* oriented along the gradient from high to low pressure. In three dimensions the acceleration γ_p from the pressure-gradient force is

$$\gamma_p = -\frac{1}{\rho}\nabla \bullet P \tag{4.4}$$

where $\nabla = (\partial/\partial x, \partial/\partial y, \partial/\partial z)$ is the gradient vector. Consider an air parcel initially at rest in a pressure-gradient field in the northern hemisphere (Figure 4-5). There is no Coriolis force applied to the air parcel since it is at rest. Under the effect of the pressure-gradient force, the air parcel begins to flow along the gradient from high to low pressure, i.e., perpendicularly to the *isobars* (lines of constant pressure). As the air parcel acquires speed, the increasing Coriolis acceleration causes it to curve to the right. Eventually, an equilibrium is reached when the Coriolis force balances the pressure-gradient force, resulting in a steady flow (zero acceleration). This steady flow is called the *geostrophic flow*. It must be parallel to the isobars, as only then is the Coriolis force exerted in the direction directly opposite of the pressure-gradient force (Figure 4-5). In the northern hemisphere, the geostrophic flow is such that the higher pressure is to the right of the flow; air flows clockwise around a center of high pressure and counterclockwise around a center of low pressure (Figure 4-6). The direction of flow is reversed in the southern hemisphere. A center

of high pressure is called an *anticyclone* or simply a *High*. A center of low pressure is called a *cyclone* or simply a *Low*.

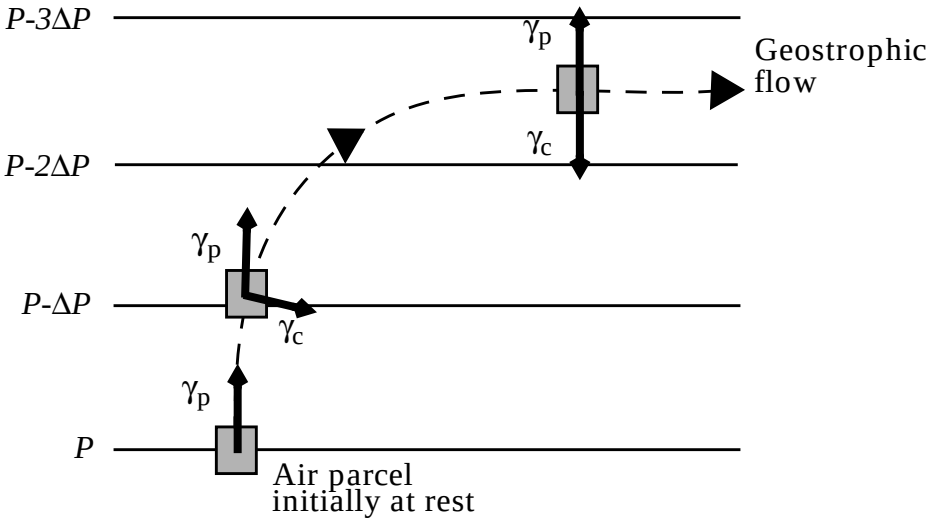

Figure 4-5 Development of geostrophic flow (northern hemisphere). An air parcel in a pressure-gradient field is subjected to a pressure-gradient acceleration (γ_p) and a Coriolis acceleration (γ_c), resulting in a flow following the dashed line. Isobars are shown as solid lines.

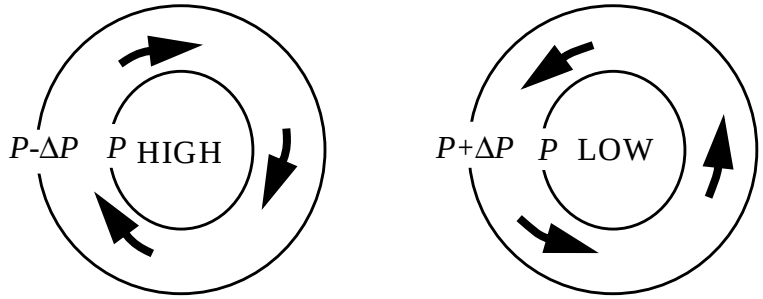

Figure 4-6 Geostrophic flows around centers of high and low pressure (northern hemisphere)

4.1.3 The effect of friction

Near the surface of the Earth, an additional horizontal force exerted on the atmosphere is the *friction force.* As air travels near the surface, it loses momentum to obstacles such as trees, buildings, or ocean waves. The friction acceleration γ_f representing this loss of momentum is exerted in the direction opposite to the direction of motion. The resulting slowdown of the flow decreases the Coriolis acceleration (equation *(4.2)*), so that the air is deflected towards the region of low pressure. This effect is illustrated by the triangle of forces in Figure 4-7. The flow around a region of high pressure is

deflected away from the High while the flow around a region of low pressure is deflected towards the Low. This result is the same in both hemispheres. In a high-pressure region, sinking motions are required to compensate for the divergence of air at the surface (Figure 4-8); as air sinks it heats up by compression, relative humidity goes down, leading to sunny and dry conditions. By contrast, in a low-pressure region, convergence of air near the surface causes the air to rise (Figure 4-8); as the air rises it cools by expansion, its relative humidity increases, and clouds and rain may result. Thus high pressure is generally associated with fair weather, and low pressure with poor weather, in both hemispheres.

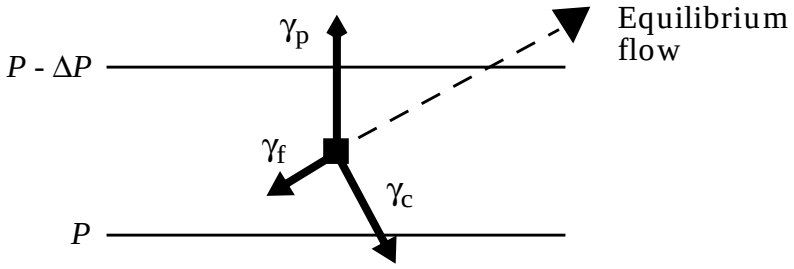

Figure 4-7 Modification of the geostrophic flow by friction near the surface.

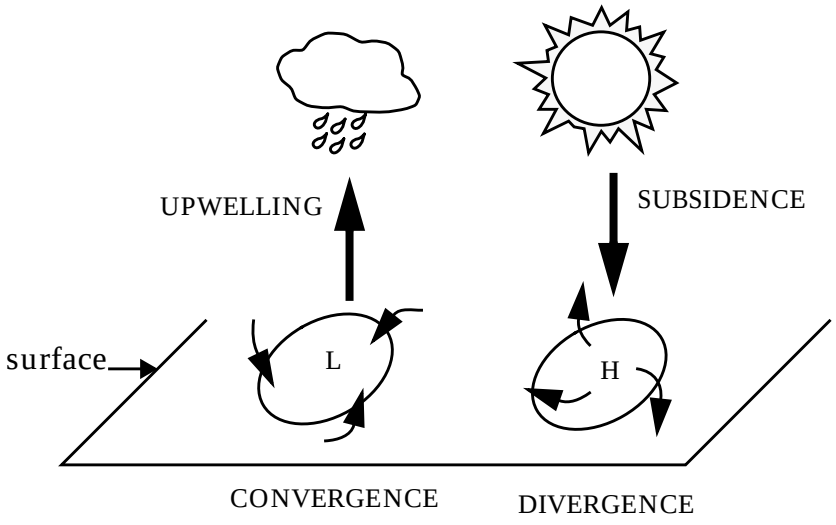

Figure 4-8 Weather associated with surface Highs and Lows

4.2 THE GENERAL CIRCULATION

Figure 4-9 shows the mean sea-level pressures and general patterns of surface winds over the globe in January and July. There are a number of prominent features:

- Near the equator, a line labeled “ITCZ” (intertropical convergence zone) identifies a ribbon of atmosphere, only a few

hundred km wide, with persistent convergence and associated clouds and rain. The clouds often extend up to the tropopause. The location of the ITCZ varies slightly with season, moving north from January to July.

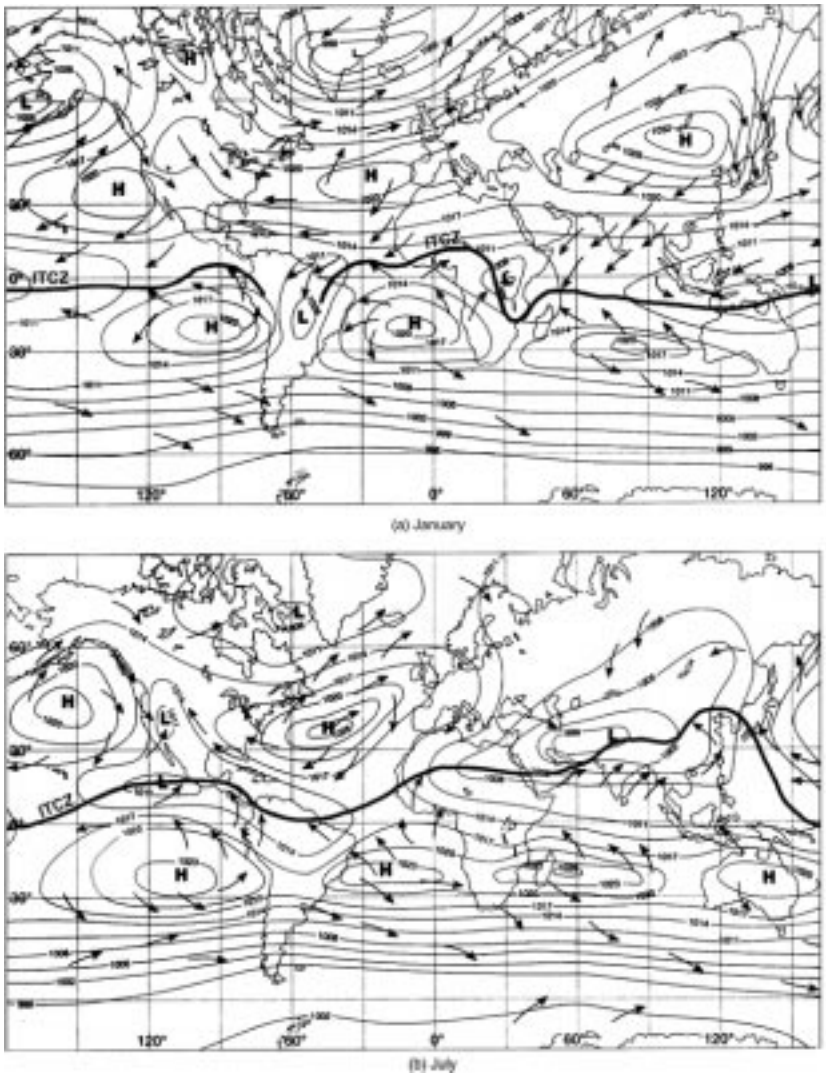

Figure 4-9 Average surface pressures and surface wind patterns in January and July. (Lutgens, F.K., and E.J. Tarbuck, *The Atmosphere, 6th ed., Prentice Hall, 1995).*

- North and south of that line, and extending to about 20^{o}-30^{o} latitude, is the tropical regime of easterly "trade winds" (one refers to "easterly winds", or "easterlies", as winds blowing from east to west).
- At about 30^{o} north and south are regions of prevailing high pressure, with centers of high pressure (subtropical anticyclones) generally over the oceans. High pressure is associated with dry conditions, and indeed one finds that the

major deserts of the world are at about 30^{o} latitude.

- At higher latitudes (mid-latitudes) the winds shift to a prevailing westerly direction. These winds are considerably more consistent in the southern hemisphere (the “roaring forties”, the“screaming fifties”) than in the northern hemisphere.

The first model for the general circulation of the atmosphere was proposed by Hadley in the 18th century and is illustrated in Figure 4-10. Hadley envisioned the circulation as a global sea breeze (section 2.5) driven by the temperature contrast between the hot equator and the cold poles.

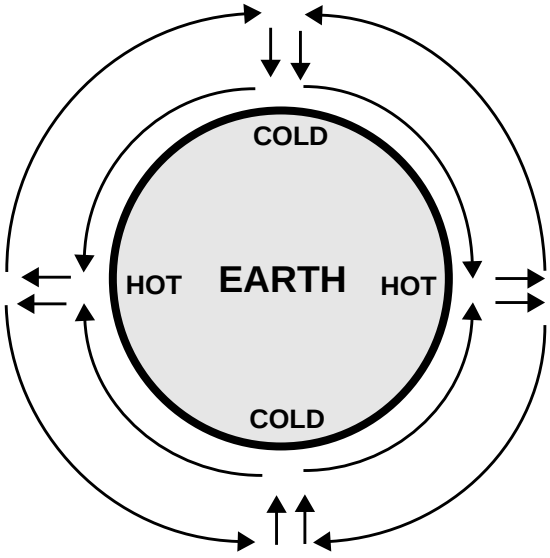

Figure 4-10 The Hadley circulation

This model explains the presence of the ITCZ near the equator and the seasonal variation in the location of the ITCZ (as the region of maximum heating follows the Sun from the southern tropics in January to the northern tropics in July). A flaw is that it does not account for the Coriolis force. Air in the high-altitude branches of the Hadley circulation cells blowing from the equator to the pole is accelerated by the Coriolis force as it moves poleward (Figure 4-11), eventually breaking down into an unstable flow. Thus it is observed that the Hadley cells extend only from the equator to about 30^{o} latitude. At 30^{o} the air is pushed down, producing the observed subtropical high-pressure belts. The Hadley cells remain a good model for the circulation of the tropical atmosphere. The Coriolis force acting on the low-altitude branches produces the easterlies observed near the surface (Figure 4-11).

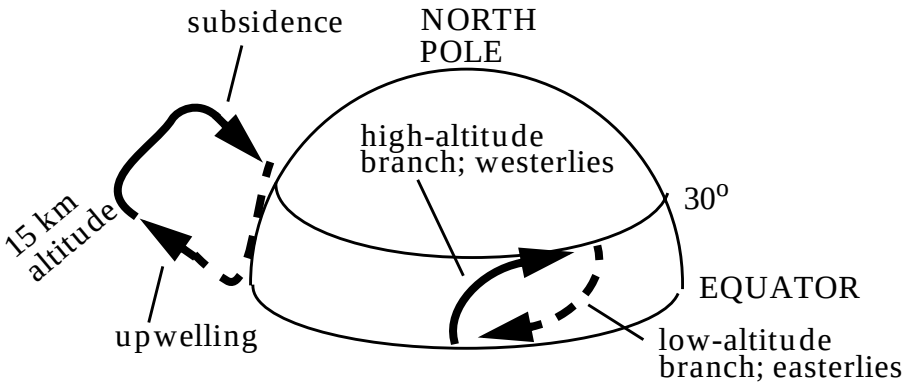

Figure 4-11 Northern hemisphere Hadley cell

As the air subsides in the subtropical anticyclones it experiences a clockwise rotation in the northern hemisphere (counterclockwise in the southern hemisphere). Further poleward transport is difficult because of the strong Coriolis force, which tends to produce a geostrophic longitudinal flow (the westerlies) by balancing the meridional pressure-gradient force. For air to move poleward it must lose angular momentum; this loss is accomplished by friction at the surface, and is more efficient in the northern hemisphere, where large land masses and mountains provide roughness, than in the southern hemisphere, where the surface is mainly ocean and relatively smooth. This difference between the two hemispheres explains the more persistent westerlies in the southern midlatitudes, and the particularly cold antarctic atmosphere.

Typical time scales for horizontal transport in the troposphere are shown in Figure 4-12. Transport is fastest in the longitudinal direction, corresponding to the geostrophic flow driven by the latitudinal heating gradient. Longitudinal wind speeds are of the order of 10 m s^{-1}, and observations show that it takes only a few weeks for air to circumnavigate the globe in a given latitudinal band. Meridional transport is slower; wind speeds are of the order of 1 m s^{-1}, and it takes typically 1-2 months for air at midlatitudes to exchange with the tropics or with polar regions. Interhemispheric transport is even slower because of the lack of thermal forcing across the Equator (recall the Hadley model in Figure 4-10). It thus takes about 1 year for air to exchange between the northern and southern hemispheres (problem 3. 4). The interhemispheric exchange of air takes place in part by horizontal mixing of convective storm outflows at the ITCZ, in part by seasonal shift in the location of the ITCZ which causes tropical air to slosh between hemispheres, and in part by breaks in the ITCZ caused for example by land-ocean circulations such as the Indian

monsoon.

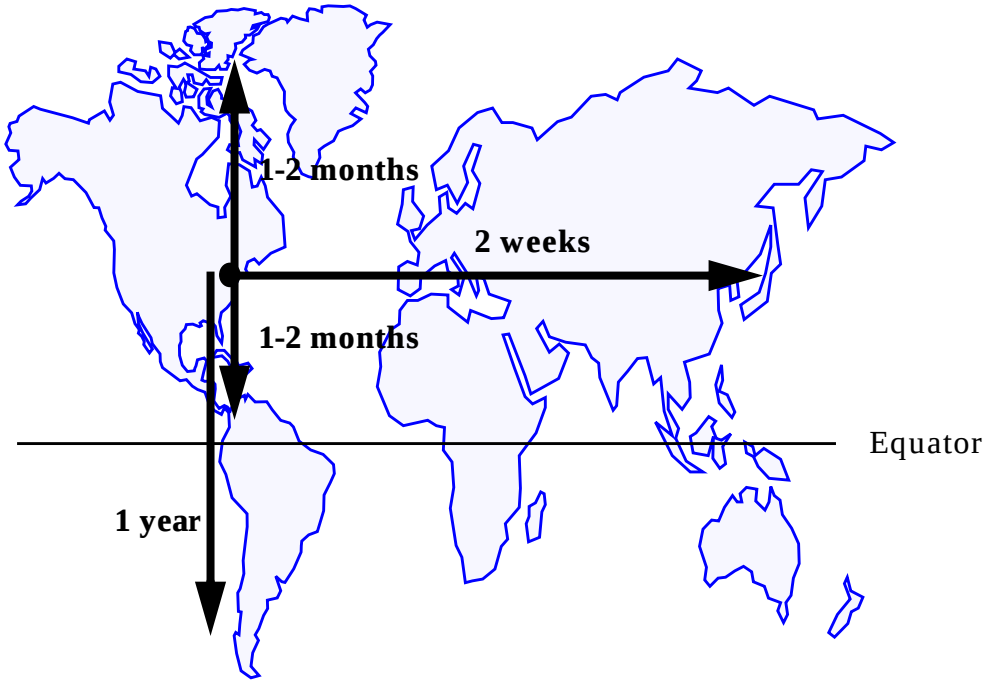

Figure 4-12 Typical time scales for global horizontal transport in the troposphere

4.3 VERTICAL TRANSPORT

So far in this chapter we have described the circulation of the atmosphere as determined by the balance between horizontal forces. Horizontal convergence and divergence of air in the general circulation induce vertical motions (Figure 4-8 and Figure 4-11) but the associated vertical wind speeds are only in the range 0.001-0.01 m s^{-1} (compare to 1-10 m s^{-1} for typical horizontal wind speeds). The resulting time scale for vertical transport from the surface to the tropopause is about 3 months. Faster vertical transport can take place by locally driven *buoyancy*, as described in this section.

4.3.1 Buoyancy

Consider an object of density ρ and volume *V* immersed in a fluid (gas or liquid) of density ρ' (Figure 4-13). The fluid pressure exerted on the top of the object is less than that exerted on the bottom; the resulting pressure-gradient force pushes the object upward, counteracting the downward force ρ*Vg* exerted on the object by gravity. The net force exerted on the object, representing the difference between the pressure-gradient force and gravity, is called the *buoyancy*.

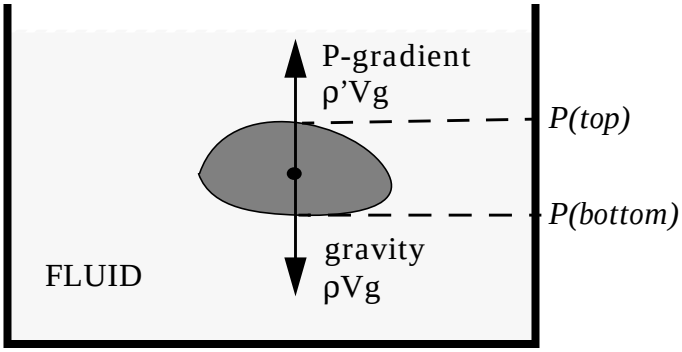

Figure 4-13 Gravity and pressure-gradient forces applied on an object (density ρ) immersed in a fluid (density ρ')

To derive the magnitude of the pressure-gradient force, imagine a situation where the immersed object has a density ρ' identical to that of the fluid (as, for example, if the "object" were just an element of the fluid). Under these circumstances there is no net force exerted upward or downward on the object; the pressure-gradient force exactly balances the gravity force ρ'*Vg*. Since the pressure-gradient force depends only on the volume of the object and not on its density, we conclude in the general case that the pressure-gradient force exerted on an object of volume *V* is given by ρ'*Vg*, and therefore that the buoyant upward force exerted on the object is (ρ' - ρ)*Vg*. The buoyant acceleration γ_b, defined as the buoyant force divided by the mass ρ*V*, is

$$\gamma_b = \frac{\rho' - \rho}{\rho} g \, . \qquad (4.5)$$

If the object is lighter than the fluid in which it is immersed, it is accelerated upward; if it is heavier it is accelerated downward.

Exercise 4-1 Buoyant motions in the atmosphere associated with local differences in heating can be vigorous. Consider a black parking lot where the surface air temperature (*T* = 301 K) is slightly warmer than that of the surrounding area (*T'* = 300 K). What is the buoyant acceleration of the air over the parking lot?

Answer. Recall that $\rho \sim 1/T$ (ideal gas law). The resulting buoyant acceleration is

$$\gamma_b = \frac{\rho' - \rho}{\rho} g = \frac{\frac{1}{T'} - \frac{1}{T}}{\frac{1}{T}} g = \left(\frac{T - T'}{T'}\right) g = 3.3\text{x}10^{-2} \text{ m s}^{-2}$$

which means that the air over the parking lot acquires an upward vertical velocity of 3.3 cm s^{-1} in one second. Compare to the vertical velocities of the order of 0.1 cm s^{-1} derived from the general circulation. Such a large acceleration arising from only a modest temperature difference illustrates the importance of buoyancy in determining vertical transport in the atmosphere.

4.3.2 Atmospheric stability

Buoyancy in the atmosphere is determined by the vertical gradient of temperature. Consider a horizontally homogeneous atmosphere with a vertical temperature profile $T_{ATM}(z)$. Let *A* represent an air parcel at altitude *z* in this atmosphere.

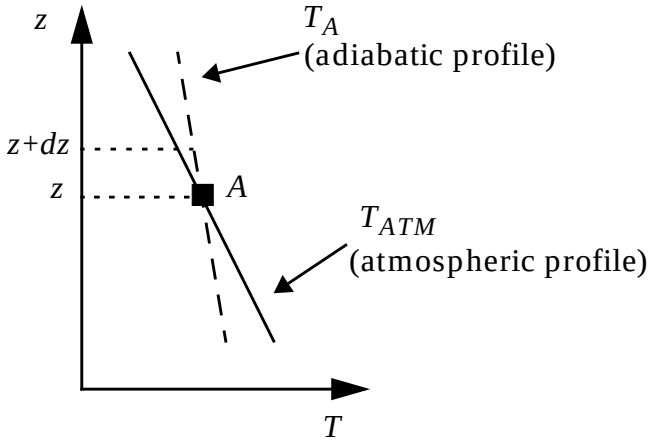

Figure 4-14 Atmospheric stability: $-dT_{ATM}/dz > -dT_A/dz$ indicates an unstable atmosphere.

Assume that by some small external force the air parcel *A* is pushed upward from *z* to *z+dz* and then released. The pressure at *z+dz* is less than that at *z*. Thus the air parcel expands, and in doing so performs work ($dW = -PdV$). Let us assume that the air parcel does not exchange energy with its surroundings as it rises, i.e., that the rise is *adiabatic* ($dQ = 0$). The work is then performed at the expense of the internal energy *E* of the air parcel: $dE = dW + dQ = -PdV < 0$. Since the internal energy of an ideal gas is a function of temperature only, the air parcel cools. This cooling is shown as the dashed line in Figure 4-14 (adiabatic profile).

One might expect that as the air parcel cools during ascent, it will become heavier than its surroundings and therefore sink back to its position of origin on account of buoyancy. However, the temperature of the surrounding atmosphere also usually decreases with altitude (Figure 4-14). Whether the air parcel keeps on rising

depends on how rapid its *adiabatic cooling rate* is relative to the change of temperature with altitude in the surrounding atmosphere. If $T_A(z+dz) > T_{ATM}(z+dz)$, as shown in the example of Figure 4-14, the rising air parcel at altitude $z+dz$ is warmer than the surrounding atmosphere at the same altitude. As a result, its density ρ is less than that of the surrounding atmosphere and the air parcel is accelerated upward by buoyancy. The atmosphere is *unstable* with respect to vertical motion, because any initial push upward or downward on the air parcel will be amplified by buoyancy. We call such an atmosphere *convective* and refer to the rapid buoyant motions as *convection*.

On the contrary, if $T_A(z+dz) < T_{ATM}(z+dz)$, then the rising air parcel is colder and heavier than the surrounding environment and sinks back to its position of origin; vertical motion is suppressed and the atmosphere is *stable*.

The rate of decrease of temperature with altitude ($-dT/dz$) is called the *lapse rate*. To determine whether an atmosphere is stable or unstable, we need to compare its *atmospheric lapse rate* $-dT_{ATM}/dz$ to the *adiabatic lapse rate* $-dT_A/dz$. Note that stability is a *local* property of the atmosphere defined by the local value of the atmospheric lapse rate; an atmosphere may be stable at some altitudes and unstable at others. Also note that stability refers to both upward and downward motions; if an atmosphere is unstable with respect to rising motions it is equivalently unstable with respect to sinking motions. Instability thus causes rapid vertical mixing rather than unidirectional transport.

4.3.3 Adiabatic lapse rate

Our next step is to derive the adiabatic lapse rate. We consider for this purpose the thermodynamic cycle shown in Figure 4-15:

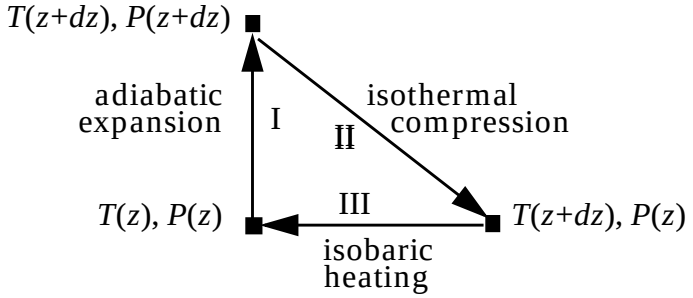

Figure 4-15 Thermodynamic cycle

In this cycle an air parcel [*T(z), P(z)*] rises adiabatically from z to $z+dz$ (process I), then compresses isothermally from $z+dz$ to z

(process II), and finally heats isobarically at altitude z (process III). The cycle returns the air parcel to its initial thermodynamic state and must therefore have zero net effect on any thermodynamic function. Consideration of the *enthalpy* (H) allows a quick derivation of the adiabatic lapse rate. The enthalpy is defined by

$$H = E + PV \tag{4.6}$$

where E is the internal energy of the air parcel. The change in enthalpy during any thermodynamic process is

$$dH = dE + d(PV) = dW + dQ + d(PV) \tag{4.7}$$

where $dW = -PdV$ is the work performed on the system and dQ is the heat added to the system. Expanding $d(PV)$ we obtain

$$dH = -PdV + dQ + PdV + VdP = dQ + VdP \tag{4.8}$$

For the adiabatic process (I), $dQ = 0$ by definition so that

$$dH_I = VdP \tag{4.9}$$

For the isothermal process (II), $dE = 0$ (the internal energy of an ideal gas is a function of temperature only) and $d(PV) = 0$ (ideal gas law), so that

$$dH_{II} = 0 \tag{4.10}$$

For the isobaric process (III), we have

$$dH_{III} = dQ = mC_P(T(z) - T(z + dz)) = -mC_P dT \tag{4.11}$$

where m is the mass of the air parcel and $C_P = 1.0 \times 10^3$ J kg^{-1} K^{-1} is the specific heat of air at constant pressure. By definition of the thermodynamic cycle,

$$dH_I + dH_{II} + dH_{III} = 0 \tag{4.12}$$

so that

$$VdP = mC_P dT \tag{4.13}$$

Replacing equation *(2.5)* and $m = \rho V$ into *(4.13)* yields the adiabatic

lapse rate (commonly denoted Γ):

$$\Gamma = -\frac{dT}{dz} = \frac{g}{C_P} = 9.8 \text{ K km}^{-1} \qquad (4.14)$$

Remarkably, Γ is a constant independent of atmospheric conditions. We can diagnose whether an atmosphere is stable or unstable with respect to vertical motions simply by comparing its lapse rate to $\Gamma = 9.8$ K km^{-1}:

$$\begin{aligned} -\frac{dT_{ATM}}{dz} &> \Gamma \quad \text{unstable} \\ -\frac{dT_{ATM}}{dz} &= \Gamma \quad \text{neutral} \\ -\frac{dT_{ATM}}{dz} &< \Gamma \quad \text{stable} \end{aligned} \qquad (4.15)$$

Particularly stable conditions are encountered when the temperature increases with altitude ($dT_{ATM}/dz > 0$); such a situation is called a *temperature inversion*.

4.3.4 Latent heat release from cloud formation

Cloudy conditions represent an exception to the constancy of Γ. Condensation of water vapor is an *exothermic* process, meaning that it releases heat (in meteorological jargon this is called *latent heat release).* Cloud formation in a rising air parcel provides an internal source of heat that partly compensates for the cooling due to expansion of the air parcel (Figure 4-16) and therefore increases its buoyancy.

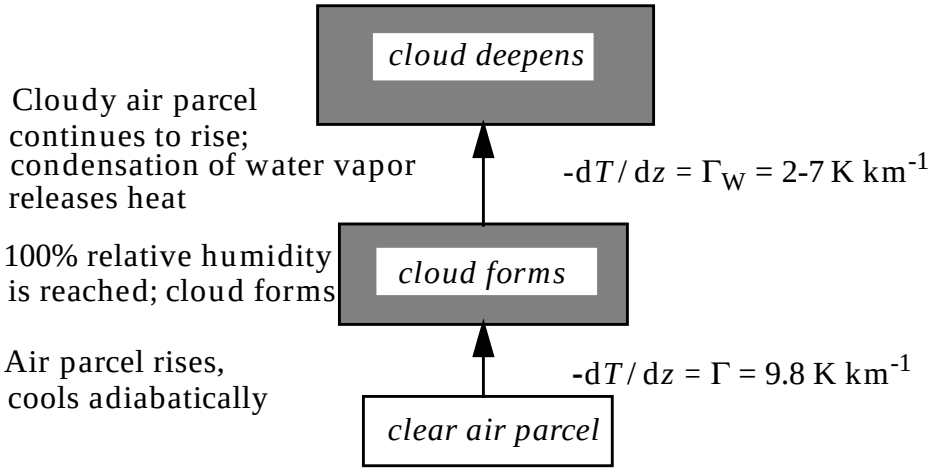

Figure 4-16 Effect of cloud formation on the adiabatic lapse rate

We refer to buoyant motions in cloud as *wet convection*. The lapse rate of a cloudy air parcel is called the *wet adiabatic lapse rate* Γ_W and ranges typically from 2 to 7 K km^{-1} depending on the water condensation rate. An atmosphere with lapse rate $\Gamma_W < -dT/dz < \Gamma$ is called *conditionally unstable*; it is stable except for air parcels that are saturated with water vapor and hence ready to condense cloudwater upon lifting (or evaporate cloudwater upon sinking).

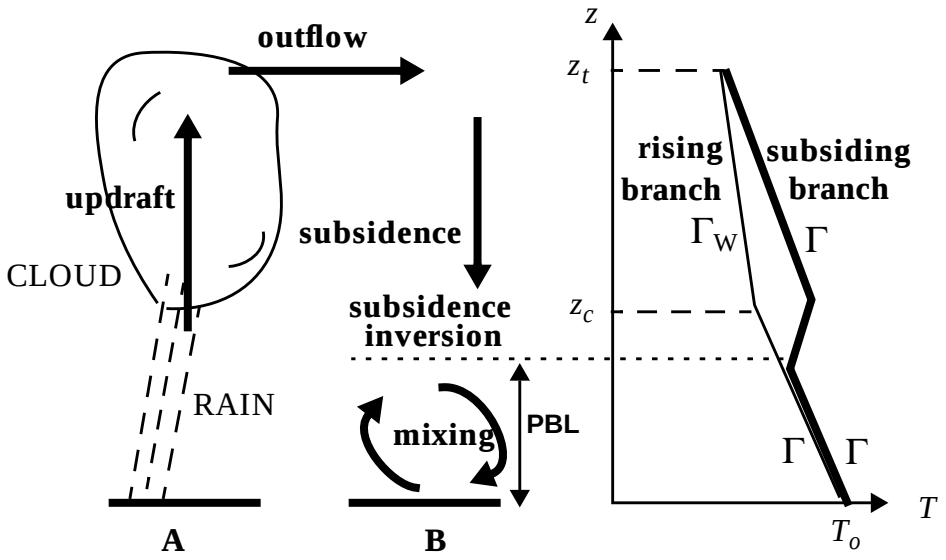

Figure 4-17 Formation of a subsidence inversion. Temperature profiles on the right panel are shown for the upwelling region A (thin line) and the subsiding region B (bold line). It is assumed for purposes of this illustration that regions A and B have the same surface temperature T_o. The air column extending up to the subsidence inversion is commonly called the planetary boundary layer (PBL).

Although cloud formation increases the buoyancy of the air parcel in which it forms, it increases the stability of the surrounding atmosphere by providing a source of heat at high altitude. This effect is illustrated in Figure 4-17. Consider an air parcel rising from the surface in an unstable atmosphere over region A. This air parcel cools following the dry adiabatic lapse rate Γ up to a certain altitude z_c at which the saturation point of water is reached and a cloud forms. As the air parcel rises further it cools following a wet adiabatic lapse rate Γ_W; for simplicity we assume in Figure 4-17 that Γ_W is constant with altitude, although Γ_W would be expected to vary as the condensation rate of water changes. Eventually, precipitation forms, removing the condensed water from the air parcel. Ultimately, the air parcel reaches an altitude z_t where it is stable with respect to the surrounding atmosphere. This altitude

(which could be the tropopause or the base of some other stable region) defines the top of the cloud. As the air parcel flows out of the cloud at altitude z_t, it has lost most of its water to precipitation.

The outflowing air is then carried by the winds at high altitude and must eventually subside for mass conservation of air to be satisfied. As the air subsides, its temperature increases following the dry adiabatic lapse rate Γ. Let us assume that the subsidence takes place over a region B that has the same surface temperature T_o as region A. For any given altitude over region B, the air subsiding from z_t is warmer than the air rising from the surface; this situation leads to stable conditions, often manifested by a *subsidence inversion* (typically at 1-3 km altitude) where the subsiding air meets the air convecting from the surface. The stability induced by subsidence is a strong barrier to buoyant motions over region B. Vertical mixing of surface air above region B is limited to the atmospheric column below the subsidence inversion; this column is commonly called the *planetary boundary layer* (PBL). Strong and persistent subsidence inversions can lead to accumulation of pollutants in the PBL over several days, resulting in air pollution episodes.

Subsidence inversions are ubiquitous in the troposphere. In their absence, air parcels heated at the surface during daytime would rise unimpeded to the tropopause, precipitating in the process. The scales involved in the upwelling and subsidence of air in Figure 4-17 (i.e., the distance between A and B) may be as short as a few km or as large as the tropical Hadley cell (compare Figure 4-11 to Figure 4-17). In the Hadley cell, air rising at the ITCZ eventually subsides in the subtropical high-pressure belts at about 30^o latitude. Persistent subsidence inversions lead to severe air pollution problems in the large subtropical cities of the world (for example Los Angeles, Mexico City, Athens, in the northern hemisphere; Sao Paulo in the southern hemisphere).

4.3.5 Atmospheric lapse rate

An atmosphere left to evolve adiabatically from an initial state would eventually achieve an equilibrium situation of neutral buoyancy where the temperature profile follows the adiabatic lapse. However, external sources and sinks of heat prevent this equilibrium from being achieved.

Major sources of heat in the atmosphere include the condensation of water vapor, discussed in the previous section, and the absorption of UV radiation by ozone. The mean lapse rate

observed in the troposphere is 6.5 K km^{-1} (Figure 2-2), corresponding to moderately stable conditions. A major reason for this stability is the release of latent heat by cloud formation, as illustrated in Figure 4-17. Another reason is the vertical gradient of radiative cooling in the atmosphere, which will be discussed in chapter 7.

Absorption of solar UV radiation by the ozone layer in the stratosphere generates a temperature inversion (Figure 2-2). Because of this inversion, vertical motions in the stratosphere are strongly suppressed (the stratosphere is stratified, hence its name). The temperature inversion in the stratosphere also provides a cap for unstable motions initiated in the troposphere, and more generally suppresses the exchange of air between the troposphere and the stratosphere. This restriction of stratosphere-troposphere exchange limits the potential of many pollutants emitted at the surface to affect the stratospheric ozone layer (problem 3. 3).

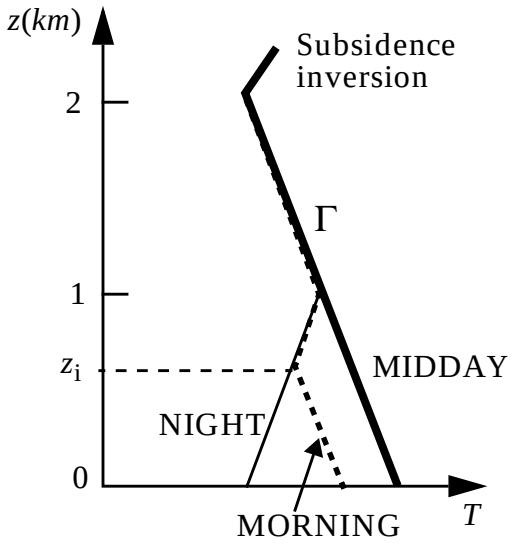

Figure 4-18 Diurnal cycle of temperature above a land surface

Heating and cooling of the surface also affect the stability of the atmosphere. As we will see in chapter 7, the Earth's surface is a much more efficient absorber and emitter of radiation than the atmosphere above. During daytime, heating of the surface increases air temperatures close to the surface, resulting in an unstable atmosphere. In this unstable atmosphere the air moves freely up and down, following the adiabatic lapse rate, so that the atmospheric lapse rate continually adjusts to Γ; unstable lapse rates are almost never actually observed in the atmosphere except in the lowest few meters above the surface, and the observation of an

adiabatic lapse rate is in fact a sure indication of an unstable atmosphere.

At sunset the land surface begins to cool, setting up stable conditions near the surface. Upward transport of the cold surface air is then hindered by the stable conditions. If winds are low, a temperature inversion typically develops near the surface as shown in Figure 4-18. If winds are strong, the cold surface air is forced upward by mechanical turbulence and moderately stable conditions extend to some depth in the atmosphere. After sunrise, heating of the surface gradually erodes the stable atmosphere from below until the unstable daytime profile is reestablished. We call the unstable layer in direct contact with the surface the *mixed layer*, and the top of the mixed layer the *mixing depth;* the mixing depth z_i for the morning profile is indicated in Figure 4-18. The mixing depth does not usually extend to more than about 3 km altitude, even in the afternoon, because of capping by subsidence inversions.

This diurnal variation in atmospheric stability over land surfaces has important implications for urban air pollution; ventilation of cities tends to be suppressed at night and facilitated in the daytime (problem 4. 4). In winter when solar heating is weak, breaking of the inversion is difficult and accumulation of pollutants may result in severe air pollution episodes (problem 4. 5).

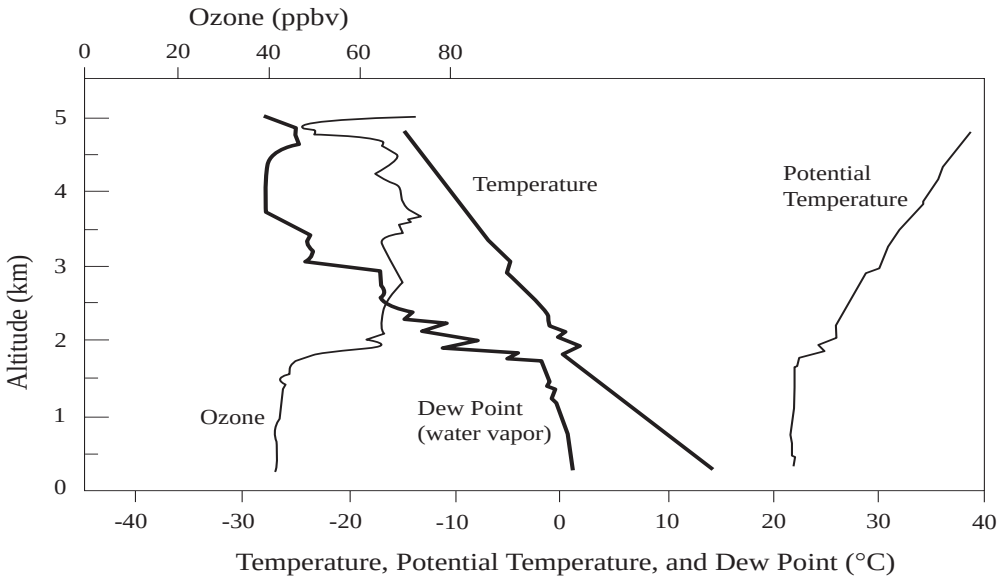

Figure 4-19 Vertical profiles of temperature *T*, potential temperature θ, water vapor (dew point), and ozone measured by aircraft in early afternoon in August over eastern Canada.

Figure 4-19 illustrates how solar heating generates an unstable mixed layer in the lower troposphere. The Figure shows vertical profiles of temperature, water vapor, and ozone measured in early afternoon in summer during an aircraft mission over eastern Canada. Water vapor is evaporated from the surface and transported upward, while ozone subsides from aloft and is destroyed by deposition to the Earth's surface (chemical complications to the interpretation of the ozone profile will be discussed in chapter 11 and are of little relevance here). Also shown in Figure 4-19 is the *potential temperature* θ, defined as the temperature that an air parcel would assume if it were brought adiabatically to 1000 hPa. The definition of θ implies that $d\theta/dz = 0$ when $dT/dz = -\Gamma$, and $d\theta/dz > 0$ when the atmosphere is stable; θ is a conserved quantity during adiabatic motions and is therefore a convenient indicator of the stability of the atmosphere.

Inspection of Figure 4-19 shows that solar heating of the surface results in an unstable mixed layer extending from the surface up to 1.7 km altitude. The unstable condition is diagnosed by $-dT/dz \approx \Gamma$, or equivalently $d\theta/dz \approx 0$. Water vapor and ozone are nearly uniform in the mixed layer, reflecting the intensity of vertical mixing associated with the unstability of the atmosphere. At about 1.7 km altitude, a small subsidence inversion is encountered where the temperature increases by about 2 K. Although small, this inversion produces sharp gradients in water vapor and ozone reflecting the strong barrier to vertical transport. Above that inversion the atmosphere is moderately stable ($-dT/dz > 0$, but $d\theta/dz > 0$), resulting in substantial structure in the water vapor and ozone profiles; the poor vertical mixing allows these structures to be maintained. A second weak inversion at 3 km altitude is associated with amother sharp drop in water vapor. An important message from Figure 4-19 is that the vertical structure of atmospheric composition is highly dependent on atmospheric stability.

4.4 TURBULENCE

So far we have discussed the role of buoyancy in driving vertical motions in the atmosphere, but we have yet to quantify the rates of vertical transport. As pointed out in section *4.3.2*, buoyancy in an unstable atmosphere accelerates both upward and downward motions; there is no preferred direction of motion. One observes considerable irregularity in the vertical flow field, a characteristic known as *turbulence*. In this section we describe the turbulent nature of atmospheric flow, obtain general expressions for calculating turbulent transport rates, and infer characteristic times for vertical transport in the atmosphere.

4.4.1 Description of turbulence

There are two limiting regimes for fluid flow: *laminar* and *turbulent*. Laminar flow is smooth and steady; turbulent flow is irregular and fluctuating. One finds empirically (and can justify to some extent theoretically) that whether a flow is laminar or turbulent depends on its dimensionless *Reynolds number Re*:

$$Re = \frac{UL}{\vartheta} \tag{4.16}$$

where U is the mean speed of the flow, L is a characteristic length defining the scale of the flow, and ϑ is the *kinematic viscosity* of the fluid ($\vartheta = 1.5 \times 10^{-5}$ m^{-2} s^{-1} for air). The transition from laminar to turbulent flow takes place at Reynolds numbers in the range 1000-10,000. Flows in the atmosphere are generally turbulent because the relevant values of U and L are large. This turbulence is evident when one observes the dispersion of a combustion plume emanating from a cigarette, a barbecue, or a smokestack.

4.4.2 Turbulent flux

Consider a smokestack discharging a pollutant X (Figure 4-20). We wish to determine the vertical flux F of X at some point M downwind of the stack. The number of molecules of X crossing an horizontal surface area dA centered on M during time dt is equal to the number $n_X wdtdA$ of molecules in the volume element $wdtdA$, where w is the vertical wind velocity measured at point M and n_X is the number concentration of X. The flux F (molecules cm^{-2} s^{-1}) at point M is obtained by normalizing to unit area and unit time:

$$F = \frac{n_X wdtdA}{dtdA} = n_X w = n_a C_X w \tag{4.17}$$

where n_a is the number air density of air and C_X is the mixing ratio of X. We will drop the subscript X in what follows. From equation *(4.17)*, we can determine the vertical flux F of pollutant X at point M by continuous measurement of C and w. Due to the turbulent nature of the flow, both C and w show large fluctuations with time, as illustrated schematically in Figure 4-21.

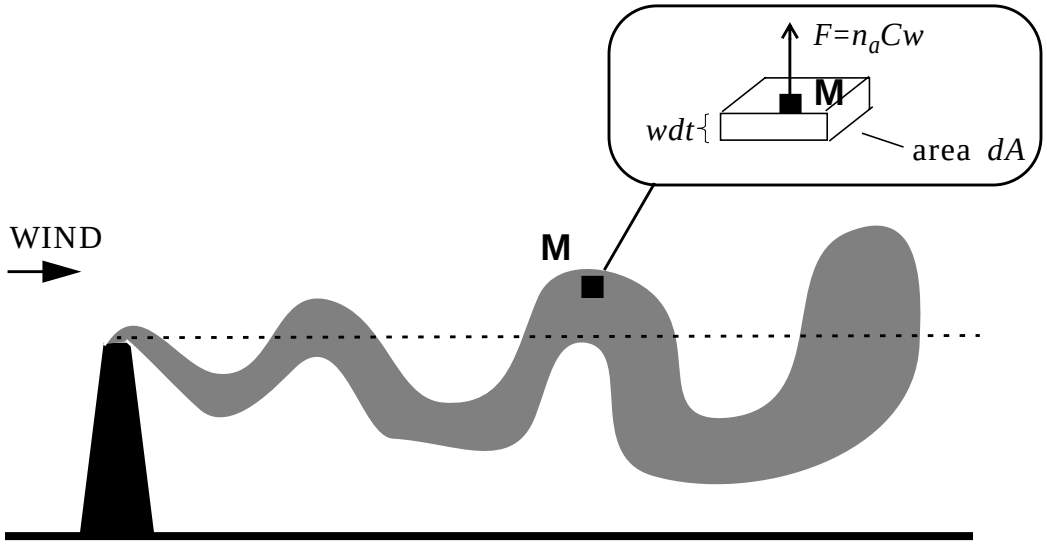

Figure 4-20 Instantaneous smokestack plume

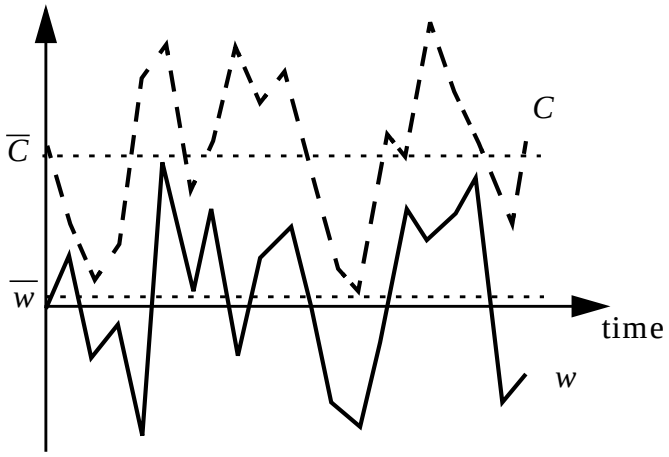

Figure 4-21 Time series of *C* and *w* measured at a fixed point *M*. $\overline{C}$ and $\overline{w}$ are the time-averaged values.

Since C and w are fluctuating quantities, so is F. We are not really interested in the instantaneous value of F, which is effectively random, but in the mean value $\overline{F} = n_a\overline{Cw}$ over a useful interval of time Δt (typically 1 hour). Let $\overline{C}$ and $\overline{w}$ represent the mean values of C and w over Δt. We decompose $C(t)$ and $w(t)$ as the sums of mean and fluctuating components:

$$\begin{aligned} C(t) &= \overline{C} + C'(t) \\ w(t) &= \overline{w} + w'(t) \end{aligned} \qquad (4.18)$$

where C' and w' are the fluctuating components; by definition, $\overline{C'} = 0$ and $\overline{w'} = 0$. Replacing *(4.18)* into *(4.17)* yields:

$$\begin{aligned} \bar{F} &= n_a(\overline{\bar{C}\bar{w} + \bar{C}w' + C'\bar{w} + C'w'}) \\ &= n_a(\bar{C}\bar{w} + \bar{C}\bar{w}' + \bar{C}'\bar{w} + \overline{C'w'}) \\ &= n_a(\bar{C}\bar{w} + \overline{C'w'}) \end{aligned} \qquad (4.19)$$

The first term on the right-hand-side, $F_A = n_a\bar{C}\ \bar{w}$, is the *mean advective flux* driven by the mean vertical wind $\bar{w}$. The second term, $F_T = n_a\overline{C'w'}$, is the *turbulent flux* driven by the covariance between C and w. The mean wind $\bar{w}$ is generally very small relative to w' because atmospheric turbulence applies equally to upward and downward motions, as discussed above. In the troposphere, F_T usually dominates over F_A in determining rates of vertical transport.

One can apply the same distinction between mean advective flux and turbulent flux to horizontal motions. Mean winds in the horizontal direction are ~1000 times faster than in the vertical direction, and are more organized, so that F_A usually dominates over F_T as long as Δt is not too large (say less than a day). You should appreciate that the distinction between mean advective flux and turbulent flux depends on the choice of Δt; the larger Δt, the greater the relative importance of the turbulent flux.

To understand the physical meaning of the turbulent flux, consider our point *M* located above the centerline of the smokestack plume. Air parcels moving upward through *M* contain higher pollutant concentrations than air parcels moving downward; therefore, even with zero mean vertical motion of *air*, there is a net upward flux of pollutants. An analogy can be drawn to a train commuting back and forth between the suburbs and the city during the morning rush hour. The train is full traveling from the suburbs to the city, and empty traveling from the city to the suburbs. Even though there is no net motion of the train when averaged over a number of trips (the train is just moving back and forth), there is a net flow of commuters from the suburbs to the city.

The use of collocated, high-frequency measurements of C and w to obtain the vertical flux of a species, as described above, is called the *eddy correlation* technique. It is so called because it involves determination of the covariance, or correlation, between the "eddy" (fluctuating) components of C and w. Eddy correlation measurements from towers represent the standard approach for

determining biosphere-atmosphere exchange fluxes of CO_2 and many other gases (Figure 4-22). Application of the technique is often limited by the difficulty of making high-quality measurements at sufficiently high frequencies (1 Hz or better) to resolve the correlation between *C'* and *w'*.

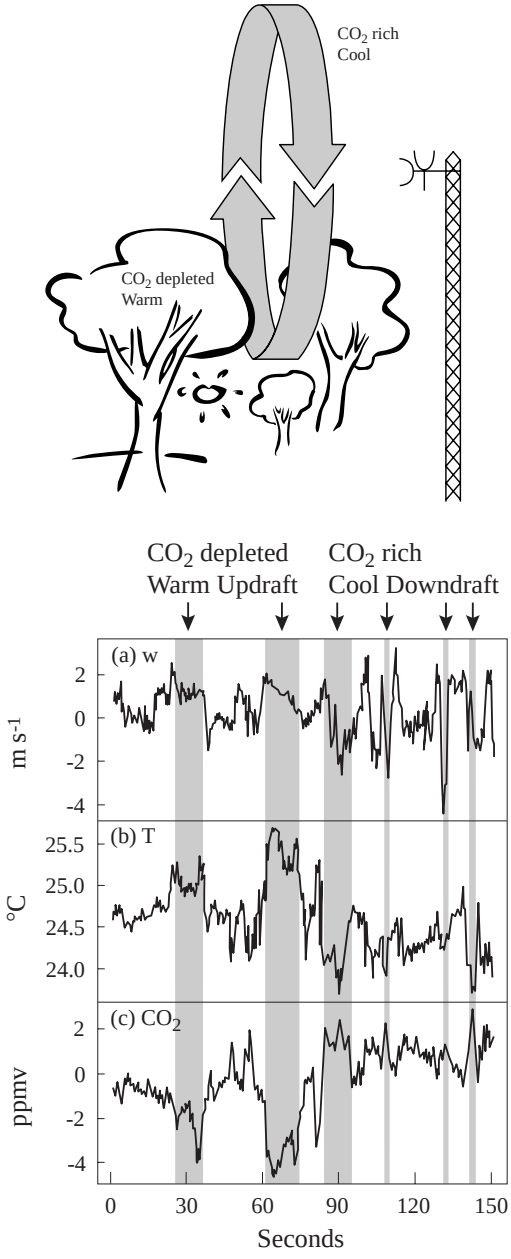

Figure 4-22 Eddy correlation measurements of CO_2 and heat fluxes made 5 m above a forest canopy in central Massachusetts. A sample 150-s time series for a summer day is shown. The canopy is a source of heat and a sink of CO_2. Air rising from the canopy ($w > 0$) is warm and CO_2-depleted, while air subsiding from aloft ($w < 0$) is cool and CO_2-enriched. Turbulent fluxes of heat and CO_2 can be obtained by correlating w with T and C_{CO2}, respectively. Figure courtesy of M. Goulden.

4.4.3 Parameterization of turbulence

So far, our discussion of atmospheric turbulence has been strictly empirical. In fact, no satisfactory theory exists to describe the characteristics of turbulent flow in a fundamental manner. In atmospheric chemistry models one must resort to empirical parameterizations to estimate turbulent fluxes. We present here the simplest and most widely used of these parameterizations.

Let us consider the smokestack plume described previously. The instantaneous plume shows large fluctuations but a time-averaged photograph would show a smoother structure (Figure 4-23):

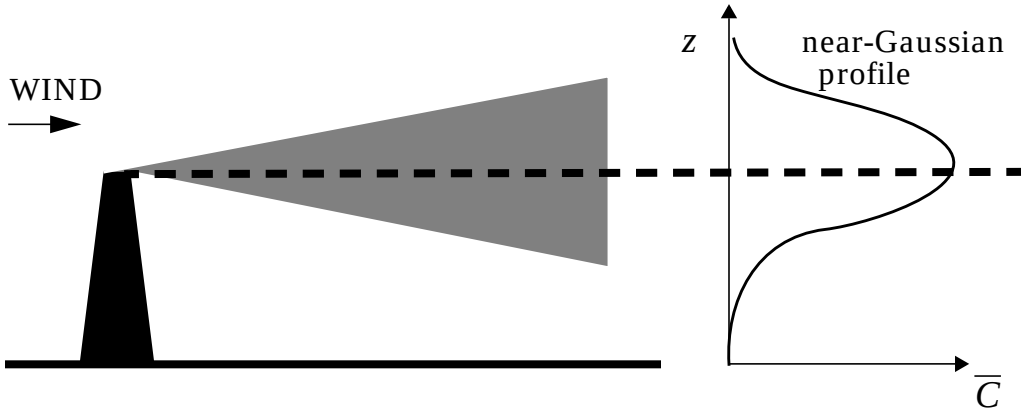

Figure 4-23 Time-averaged smokestack plume

In this time-averaged, smoothed plume there is a well-defined plume centerline, and a decrease of pollutant mixing ratios on both sides of this centerline that can be approximated as Gaussian. We draw a parallel to the Gaussian spreading in molecular diffusion, which is a consequence of the linear relationship between the diffusion flux and the gradient of the species mixing ratio (Fick's Law):

$$F = -n_a D \frac{\partial C}{\partial z} \tag{4.20}$$

Here F is the molecular diffusion flux and D ($cm^2\ s^{-1}$) is the molecular diffusion coefficient. Fick's law is the postulate on which the theory of molecular diffusion is built. Molecular diffusion is far too slow to contribute significantly to atmospheric transport (problem 4. 9), but the dispersion process resulting from turbulent air motions resembles that from molecular diffusion. We define therefore by analogy an empirical *turbulent diffusion coefficient* K_z as:

$$\bar{F} = -n_a K_z \frac{\partial \bar{C}}{\partial z} \qquad (4.21)$$

where $\bar{F}$ is now the turbulent flux and $\bar{C}$ is the time-averaged mixing ratio. Equation *(4.21)* defines the *turbulent diffusion parameterization* of turbulence.

Because K_z is an empirical quantity, it needs to be defined experimentally by concurrent measurements of $\bar{F}$ and $\partial\bar{C}/\partial z$. The resulting value would be of little interest if it did not have some generality. In practice, one finds that K_z does not depend much on the nature of the diffusing species and can be expressed with some reliability in the lower troposphere as a function of (a) the wind speed and surface roughness (which determine the mechanical turbulence arising from the collision of the flow with obstacles), (b) the heating of the surface (which determines the buoyant turbulence), and (c) the altitude (which determines the size of the turbulent eddies). Order-of-magnitude values for K_z are 10^2-10^5 cm^2 s^{-1} in a stable atmosphere, 10^4-10^6 cm^2 s^{-1} in a near-neutral atmosphere, and 10^5-10^7 cm^2 s^{-1} in an unstable atmosphere.

Exercise 4-2 We wish to determine the emission flux of the hydrocarbon isoprene from a forest canopy. Measurements from a tower above the canopy indicate mean isoprene concentrations of 1.5 ppbv at 20-m altitude and 1.2 ppbv at 30-m altitude. The turbulent diffusion coefficient is K_z = 1x10^5 cm^2 s^{-1} and the air density is 2.5x10^{19} molecules cm^{-3}. Calculate the emission flux of isoprene.

Answer. We apply equation *(4.21)*, assuming a uniform concentration gradient between 20 and 30 m altitude: $\partial C/\partial z$ = (1.2-1.5)/(30-20) = -0.03 ppbv m^{-1}. Using SI units, we obtain:

F = -1x10^{1}x2.5x10^{25}x(-0.03x10^{-9}) = 7.5x10^{15} molecules m^{-2} s^{-1}

The flux is positive (directed upward).

4.4.4 Time scales for vertical transport

The turbulent diffusion parameterization of turbulence can be used to estimate time scales for vertical transport in the troposphere

(Figure 4-24). We wish to know the mean time Δt required by an air molecule to travel a vertical distance Δz. Einstein's equation for molecular diffusion (derived from Fick's law, *(4.20)*) gives

$$\Delta t = \frac{(\Delta x)^2}{2D} \tag{4.22}$$

where Δx is the distance traveled in any direction over time Δt (molecular diffusion is isotropic). Within the context of the turbulent diffusion parameterization we can apply the Einstein equation to vertical turbulent motions in the atmosphere, replacing Δx by Δz and D by K_z:

$$\Delta t = \frac{(\Delta z)^2}{2K_z} \tag{4.23}$$

A mean value for K_z in the troposphere is about 2×10^5 cm^2 s^{-1} (problem 5. 1). Replacing into *(4.22)*, we find that it takes on average about one month for air to mix vertically from the surface to the tropopause ($\Delta z \sim 10$ km); species with lifetimes longer than a month tend to be well mixed vertically in the troposphere, while species with shorter lifetimes show large vertical gradients. Mixing within the PBL ($\Delta z \sim 2$ km) takes 1-2 days, while ventilation of the PBL with air from the middle troposphere ($\Delta z \sim 5$ km) takes on average about one week. Vertical mixing of the unstable mixed layer produced by solar heating of the surface requires less than one hour. As seen in section 4.3.5 the depth of this mixed layer varies diurnally and peaks typically at 1-2 km in the afternoon (problem 4. 4).

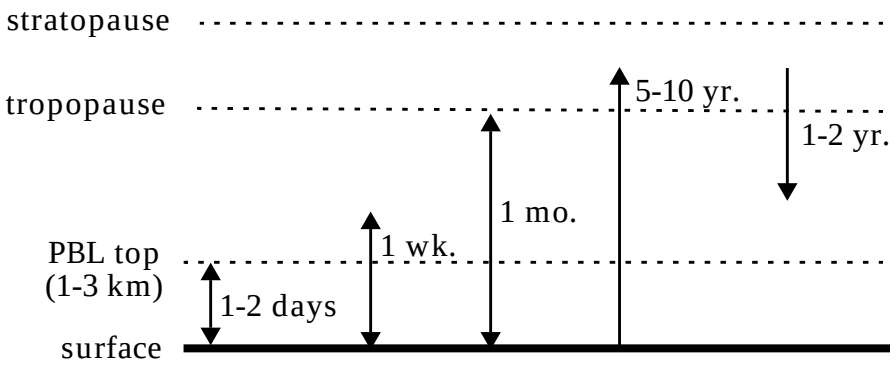

Figure 4-24 Characteristic time scales for vertical transport

Exchange of air between the troposphere and the stratosphere is considerably slower than mixing of the troposphere because of the temperature inversion in the stratosphere. It takes 5-10 years for air

from the troposphere to be transported up to the stratosphere, and 1-2 years for air from the stratosphere to be transported down to the troposphere (problem 3. 3). Air is transported from the troposphere to the stratosphere principally in the tropics, and is returned from the stratosphere to the troposphere principally at midlatitudes, but the mechanisms involved are still not well understood.

Exercise 4-3 The molecular diffusion coefficient of air at sea level is 0.2 cm^2 s^{-1}. How long on average does it take an air molecule to travel 1 m by molecular diffusion? to travel 10 m?

Answer. Using equation *(4.22)* with $D = 0.2\ cm^2\ s^{-1} = 2x10^{-5}\ m^2\ s^{-1}$, we find that the time required to travel $\Delta x = 1$ m is $\Delta t = (\Delta x)^2 / 2D = 1/(2x2x10^{-5}) = 6.9$ hours. The time required to travel 10 m is 690 hours or about 1 month! Molecular diffusion is evidently unimportant as a means of atmospheric transport and mixing at sea level. It becomes important only above about 100 km altitude (problem 4. 9).

Further reading:

Holton, J.R., *An Introduction to Dynamic Meteorology***, 2nd ed., Academic Press, New York, 1979.** Coriolis force, geostrophic flow, general circulation.

Seinfeld, J.H., and S.N. Pandis, *Atmospheric Chemistry and Physics,* **Wiley, New York, 1998.** Atmospheric stability, turbulence.